

PCCP

Accepted Manuscript



This is an *Accepted Manuscript*, which has been through the Royal Society of Chemistry peer review process and has been accepted for publication.

Accepted Manuscripts are published online shortly after acceptance, before technical editing, formatting and proof reading. Using this free service, authors can make their results available to the community, in citable form, before we publish the edited article. We will replace this *Accepted Manuscript* with the edited and formatted *Advance Article* as soon as it is available.

You can find more information about *Accepted Manuscripts* in the [Information for Authors](#).

Please note that technical editing may introduce minor changes to the text and/or graphics, which may alter content. The journal's standard [Terms & Conditions](#) and the [Ethical guidelines](#) still apply. In no event shall the Royal Society of Chemistry be held responsible for any errors or omissions in this *Accepted Manuscript* or any consequences arising from the use of any information it contains.

Cite this: DOI: 10.1039/c0xx00000x

www.rsc.org/xxxxxx

FULL PAPER

Sulfone-based electrolytes for aluminium rechargeable batteries

Yuri Nakayama,^{*a} Yui Senda,^a Hideki Kawasaki,^b Naoki Koshitani,^a Shizuka Hosoi,^a Yoshihiro Kudo,^a Hiroyuki Morioka^a and Masayuki Nagamine^a

Received (in XXX, XXX) Xth XXXXXXXXX 20XX, Accepted Xth XXXXXXXXX 20XX

DOI: 10.1039/b000000x

Electrolyte is a key material for success in the research and development of the next-generation rechargeable batteries. Aluminium rechargeable batteries that use the aluminium (Al) metals as anode materials have been an attractive candidate for the next-generation batteries, though they have not been developed yet due to the lack of practically useful electrolytes. Here we present, for the first time, non-corrosive reversible Al electrolytes working at room temperature. The electrolytes are composed of aluminium chlorides, dialkylsulfones, and dilutants, which are realized by the identification of electrochemically active Al species, the study of sulfone dependences, the effects of aluminium chlorides concentrations, dilutions and their optimizations. The characteristic feature of these materials is the lower chloride concentrations in the solutions than those in the conventional Al electrolytes, which allows us to use the Al metal anodes without corrosions. We anticipate that the sulfone-based electrolytes will open the doors for the research and development of Al rechargeable batteries.

Introduction

Research and development of rechargeable batteries having energy densities beyond the theoretical limit of Lithium-ion batteries is one of the most important issues of the present science and technologies.^{1,2} Changing the electrode materials is a promising strategy to overcome the limit. Al metal has been an attractive candidate for the anode material of a next-generation rechargeable battery because of its high capacity, moderate electrochemical activity, as well as the natural abundance.³ However stability of oxide material on the Al surface is a crucial problem especially for the reversibility, causing a large over potential or passivation phenomena. It is well known that, from some ionic liquids, such as a mixture of aluminium chloride (AlCl₃) and 1-ethyl-3-methylimidazolium chloride (EMICl) with the molar ratio greater than AlCl₃/EMICl > 1, Al can be deposited electrochemically at room temperature.⁴ Although there have been some reports on the demonstration of Al rechargeable batteries using the ionic liquids,⁵ they cannot be directly commercialized since even stainless steels get corrosion in the electrolyte solutions due to their high acidities or chloride concentrations.^{6,7}

On the other hand, there has been some reports for the electrolytes consisting of AlCl₃ and dialkylsulfone (RR'SO₂, where R and R' indicate alkyl groups) as solvent that enables Al deposition and dissolution with heating at temperatures in the range of 40-150°C.^{8,9} An attractive feature of the electrolytes is lower AlCl₃ concentrations than that in the conventional ionic liquids, indicating the possibility of Al electrolytes without both corrosion and heating when we could reduce the operating temperature. Here we present the state of the art of the sulfone-

based Al electrolytes (AlCl₃/RR'SO₂), which has been realized by studying the active ionic species in the solutions, dialkylsulfone-dependence, influence of AlCl₃ concentrations, effects of dilutions and their optimizations. And as a consequence, practical Al electrolytes operating at room temperature without corrosion have been successfully obtained.

Experimental section

All chemical preparations and measurements were performed under inert atmosphere (pure argon). Solutions of AlCl₃/RR'SO₂ = 1/4(mol) as well as other compositions were synthesized by slowly adding AlCl₃ to solvents with stirring at room temperature (25 ± 2°C). By mixing AlCl₃ and EMICl at 60 °C for 12h, an ionic liquid of AlCl₃/EMICl = 2/1(mol) was prepared. In addition, Al(BF₄)₃/EiPS = 1/8 was prepared as the supernatant liquid by precipitating the chloride as silver chloride (AgCl) by introducing an appropriate amount of silver tetrafluoroborate (AgBF₄) into AlCl₃/EiPS = 1/8(mol). Inductively coupled plasma measurements showed the composition of the electrolyte as Al/Cl/Ag/B = 1.0/1.2 × 10⁻³/8.0 × 10⁻²/3.1, confirming the removal of both chloride and silver.

²⁷Al-NMR spectra were observed with a JEOL JNM-AL400 (400 MHz) at 104.1 MHz without a deuterium lock. ²⁷Al chemical shifts are determined relative to external reference 0.5mol/l Al(NO₃)₃ in D₂O. Al K-edge X-ray absorption fine structure (XAFS) measurements were carried out in the fluorescence mode at BL-11A in KEK-PF, Tsukuba, Japan.¹⁰ Electrolyte solutions were sealed in the originally designed high vacuum compatible cells that have the polymer coated beryllium foil windows.¹¹ They were transferred into a vacuum chamber where the pressure was kept at ~10⁻⁷ torr. Individual spectra were

recorded in the energy range from 1510 to 1830 eV for Al K edge. An Al metal foil and Al_2O_3 powders were also measured to correct the energy scales of the experiments.

Electrochemical properties of the solutions were investigated by cyclic voltammetry (CV) measurements with the three electrode cell consisting of a molybdenum working electrode and Al counter and reference electrodes. A potentiostat (Solartron 1287) was used for the measurements with the scan rate of 10 mV/s. Specific conductivities were measured for each electrolyte using stainless steels two electrode cells at 10kHz with an impedance analyzer (Solartron 1260).

FT-IR spectra of various Al electrolytes were recorded at $T = 25^\circ\text{C}$ in the transmittance mode, in the wavenumber range of $1500\text{--}400\text{ cm}^{-1}$, using Nicolet Magna IR 760 spectrometer equipped with a deuterium triglycine sulphate (DTGS) detector. Solutions were sealed in liquid cells with silicon windows, being prepared in a globe box under argon atmosphere.

Electrodepositions of Al were performed by two-electrodes cells using well-polished Al electrodes with the current densities of $0.02\text{--}0.5\text{ mAcm}^{-2}$. Stainless steel strips were soaked in Al electrolytes for 24 hours to check their corrosion properties. SEM-EDX observations were performed to investigate the morphology changes of the electrode surfaces.

Results and discussions

Aluminium complexes

It has been reported that three Al species, AlCl_4^- , Al_2Cl_7^- , $\text{Al}(\text{RR}'\text{SO}_2)_3^{3+}$, are formed in $\text{AlCl}_3/\text{RR}'\text{SO}_2$,⁸ though the role of each Al complexes has not been identified clearly. So first of all, we tried to elucidate the Al species responsible for the electrochemical activities of sulfone-based Al electrolytes. We choose ethyl iso-propyl sulfone ($\text{C}_2\text{H}_5\text{-i}(\text{C}_3\text{H}_7)\text{SO}_2$: EiPS) for a starting solvent, as it is usually in a liquid state at room temperature ($T = 25^\circ\text{C}$). Then using EiPS, a standard electrolyte was prepared as $\text{AlCl}_3/\text{EiPS} = 1/4$ (mol). And we also used a conventional ionic liquid electrolyte $\text{AlCl}_3/\text{EMICl} = 2/1$ (mol) for a reference sample. In addition, in order to understand the role of Al cation $\text{Al}(\text{EiPS})_3^{3+}$, a solution without chloride was prepared by removing chlorides as AgCl precipitation, which is to be denoted as $\text{Al}(\text{BF}_4)_3/\text{EiPS} = 1/8$ (mol) hereafter.

^{27}Al NMR spectra observed for the three electrolytes are shown in Fig. 1a. It is confirmed that $\text{AlCl}_3/\text{EiPS}=1/4$ includes both AlCl_4^- ($\delta = 103\text{ ppm}$) and $\text{Al}(\text{EiPS})_3^{3+}$ ($\delta = -17\text{ ppm}$) at room temperature. It is also elucidated that $\text{AlCl}_3/\text{EMICl}=2/1$ shows a broad peak at $\delta = 105\text{ ppm}$ corresponding to the equilibrium between AlCl_4^- and Al_2Cl_7^- ,^{4,12} while $\text{Al}(\text{BF}_4)_3/\text{EiPS}=1/8$ has a peak at $\delta = -17\text{ ppm}$ corresponding to $\text{Al}(\text{EiPS})_3^{3+}$.⁸ These results are also confirmed by XAFS measurements.

On the other hand, when we raise the temperatures of $\text{AlCl}_3/\text{EiPS} = 1/4$, Al_2Cl_7^- ($\delta = 92\text{ ppm}$) appears with decreasing AlCl_4^- as shown in Fig. 1b. The relative peak intensities are summarized in Fig. 1c, where we can see the strong correlation between AlCl_4^- and Al_2Cl_7^- , indicating that there's an equilibrium in this solution presented by equation (1).^{6,13}

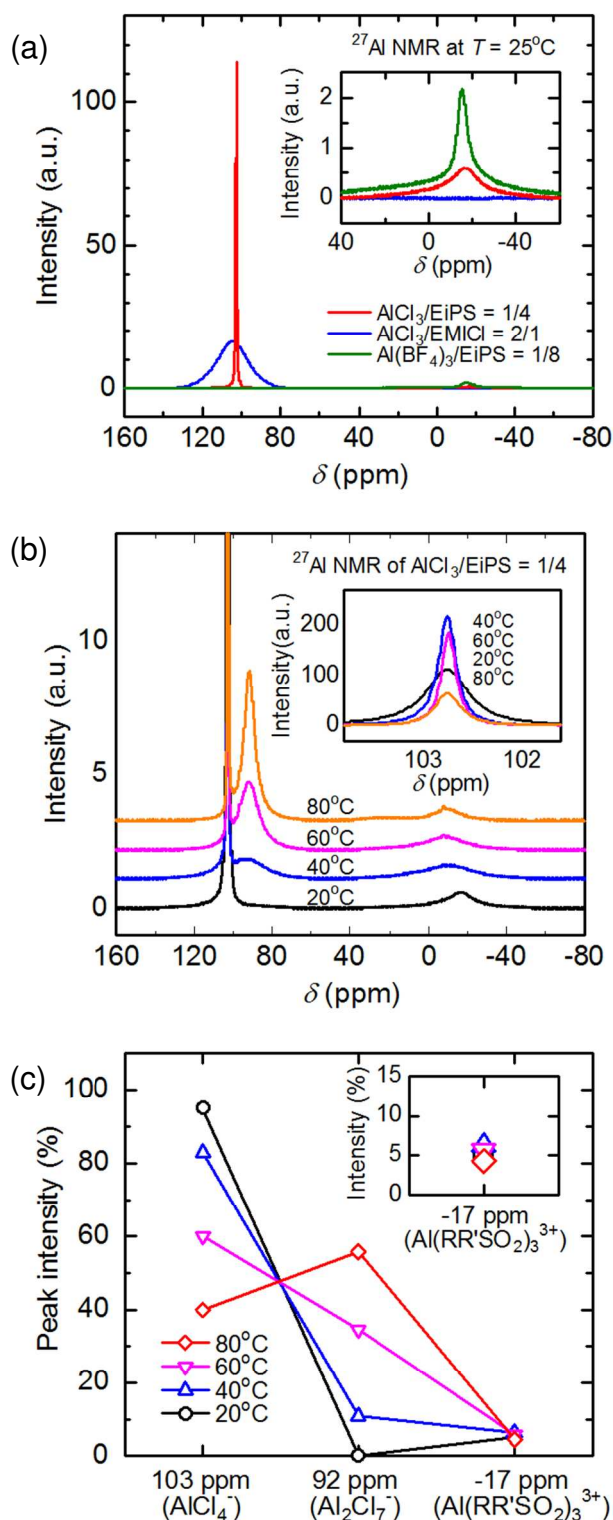


Fig.1 ^{27}Al NMR spectra of various Al electrolytes and involved Al species. (a) ^{27}Al NMR spectra of $\text{AlCl}_3/\text{EiPS} = 1/4$ (red), $\text{AlCl}_3/\text{EMICl} = 2/1$ (blue), and $\text{Al}(\text{BF}_4)_3/\text{EiPS} = 1/8$ (green), observed at $T = 25^\circ\text{C}$. The inset shows an enlargement at $\delta = -17\text{ ppm}$. (b) ^{27}Al NMR spectra of $\text{AlCl}_3/\text{EiPS} = 1/4$ measured at various temperatures, where peaks correspond to AlCl_4^- (103 ppm), Al_2Cl_7^- (92 ppm), and $\text{Al}(\text{EiPS})_3^{3+}$ (-17 ppm). The inset shows an enlargement at $\delta = 103\text{ ppm}$. (c) Relative peak intensities at $\delta = 103\text{ ppm}$, 92 ppm , and -17 ppm observed at various temperatures extracted from Fig.1b.

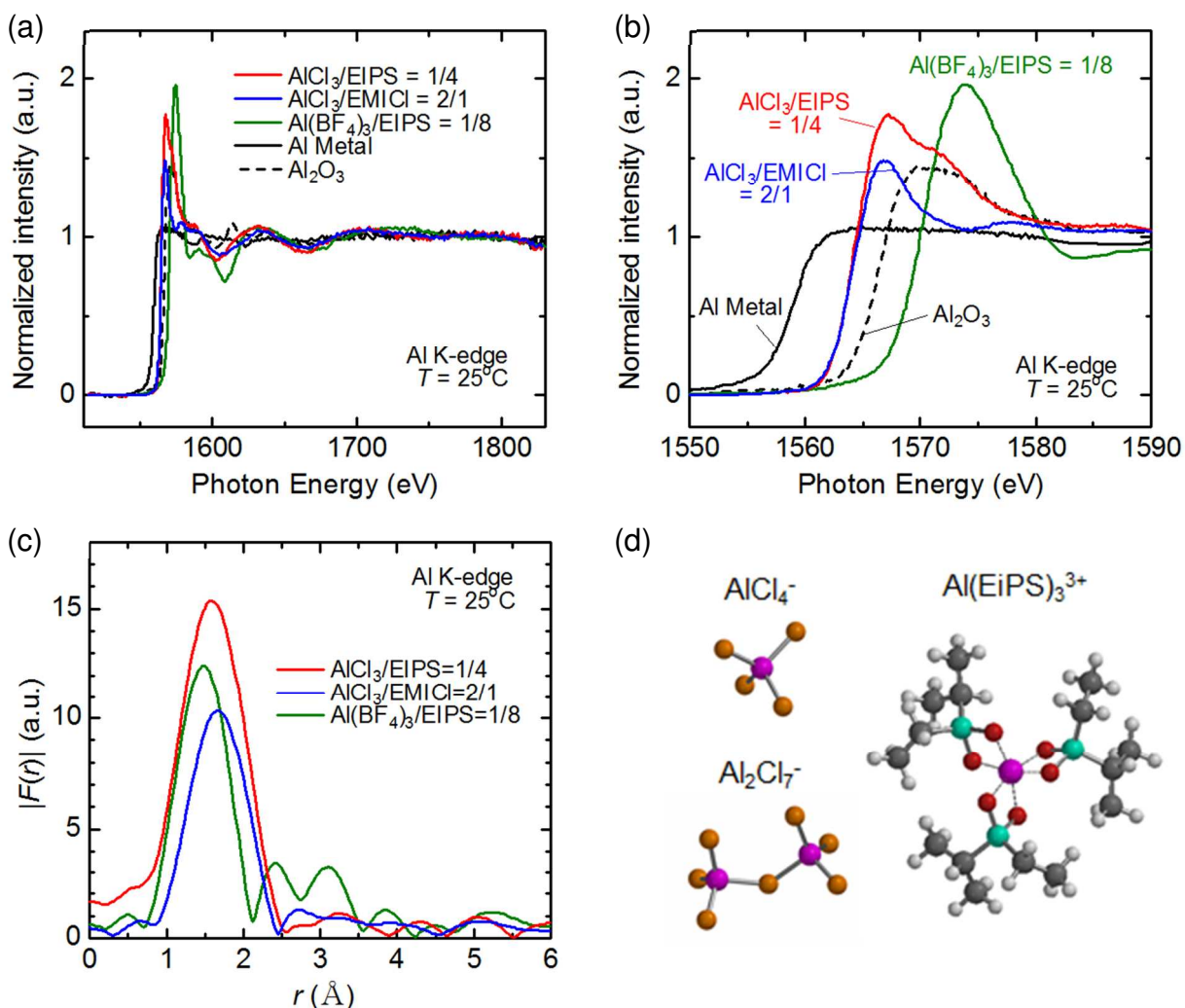


Fig.2 XAFS and XANES spectra, and Fourier transforms of EXAFS functions for various Al electrolytes. (a) Normalized XAFS spectra and (b) XANES spectra at the Al K-edge of $\text{AlCl}_3/\text{EiPS} = 1/4$ (red), $\text{AlCl}_3/\text{EMICl} = 2/1$ (blue), and $\text{Al}(\text{BF}_4)_3/\text{EiPS} = 1/8$ (green), observed at $T = 25^\circ\text{C}$. Spectra for Al metal and alumina (Al_2O_3) are also plotted as references. (c) Fourier transforms of EXAFS functions extracted from the spectra in Fig. 2a. (d) Three Al ionic species involved in the sulfone-based Al electrolyte, $\text{AlCl}_3/\text{EiPS} = 1/4$.

It should be noted that peak intensities for $\text{Al}(\text{EiPS})_3^{3+}$ ($\delta = -17$ ppm) are almost independent of temperature.

Figures 2 show (a) XAFS spectra at Al-K edge, (b) X-ray absorption near edge structures (XANES), and (c) Fourier transforms of extended XAFS (EXAFS) functions extracted from Fig. 2a. We can see that in the Fig. 2b, $\text{AlCl}_3/\text{EiPS} = 1/4$ has the absorption edge at 1563 eV (with the normalized intensity ~ 0.5) as well as the shoulder at 1572 eV, both of which corresponds to Al-Cl and Al-O bindings respectively, confirming the NMR result that AlCl_4^- and $\text{Al}(\text{EiPS})_3^{3+}$ are involved in the solution. Regarding $\text{Al}(\text{BF}_4)_3/\text{EiPS} = 1/8$, it has been found that the oxidation state of Al is much higher than that of Al_2O_3 (Fig. 2b). This is due to the strong Al-O bindings in $\text{Al}(\text{EiPS})_3^{3+}$ whose structure was confirmed for the first time in Fig. 2c as six coordination with three bidentate ligands of EiPS, where we can see the 1st peak at shorter distance (Al-O) than that of $\text{AlCl}_3/\text{EMICl} = 2/1$ (Al-Cl), as well as the 2nd and 3rd peaks in the radial structure function. As a consequence, three Al complexes are presented in Fig. 2d that are involved in $\text{AlCl}_3/\text{EiPS} = 1/4$.

Electrochemically active species

We measured CV to see the electrochemical activities of each electrolyte (Fig. 3). $\text{AlCl}_3/\text{EiPS} = 1/4$ shows reversible Al deposition and dissolution at 70°C , while we cannot see anything at room temperature (25°C). Recalling the temperature dependence of ^{27}Al -NMR spectra in Fig. 1b, emergence of Al_2Cl_7^- seems responsible for the electrochemical activity. Comparing CV spectra between $\text{AlCl}_3/\text{EiPS} = 1/4$ (70°C) and $\text{AlCl}_3/\text{EMICl} = 2/1$ (25°C), we can see some over potentials only in the former, which is due to the smaller concentration of active Al species (to be elucidated later). And it should be noted that $\text{Al}(\text{BF}_4)_3/\text{EiPS} = 1/8$ shows nothing even at 70°C , which means that $\text{Al}(\text{EiPS})_3^{3+}$ is not an electrochemically active species in itself (See Fig. S1 in supporting information). This is consistent to our XAFS results showing the stability of $\text{Al}(\text{EiPS})_3^{3+}$, though it is contrary to the previous reports.⁸ These results lead to a conclusion that the Al complex Al_2Cl_7^- is responsible for the electrochemical activities in the sulfone-based Al electrolytes.

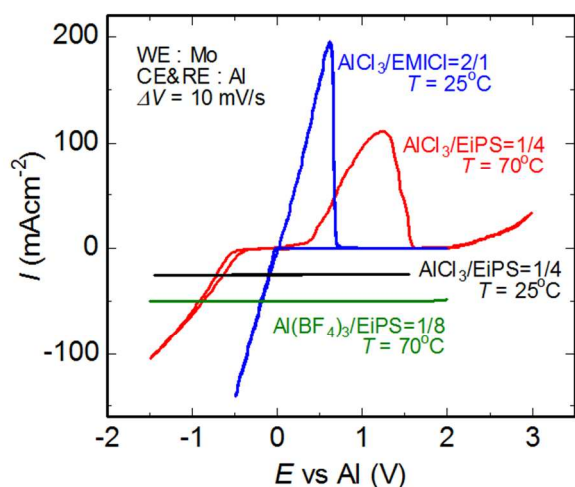
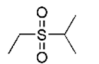
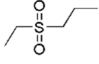
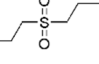
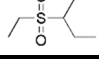


Fig.3 CV curves of $\text{AlCl}_3/\text{EiPS} = 1/4$ (red and black for $T = 70^\circ\text{C}$ and 25°C), $\text{AlCl}_3/\text{EMICl} = 2/1$ (blue, $T = 25^\circ\text{C}$), and $\text{Al}(\text{BF}_4)_3/\text{EiPS} = 1/8$ (green, $T = 70^\circ\text{C}$).

Table 1 Molecular structures, weights and melting points of various dialkylsulfones.¹³

Sulfones	M.W.	M.P.(°C)	Phase@25°C
EiPS 	136.21	< -20	Liquid
EnPS 	136.21	20-30	Liquid/Solid
DnPS 	150.24	30.5	Solid
EsBS 	150.24	-60	Liquid

M.W.: Molecular Weights, M.P.: Melting Points.

Dialkylsulfone dependence

Secondly, we tried to investigate the influence of dialkylsulfones on the electrochemical properties. Table 1 shows the four sulfones used in this study,¹⁴ EiPS, ethyl n-propyl sulfone ($\text{C}_2\text{H}_5\text{-n}(\text{C}_3\text{H}_7)\text{SO}_2$: EnPS), di-n-propyl sulfone ($\text{n}(\text{C}_3\text{H}_7)_2\text{SO}_2$: DnPS), and ethyl secondary-butyl sulfone ($\text{C}_2\text{H}_5\text{-s}(\text{C}_4\text{H}_9)\text{SO}_2$: EsBS), where we can see the different molecular structures and some properties depending on the alkyl groups. ²⁷Al-NMR spectra and the relative peak intensities, as well as CV curves observed at $T = 80^\circ\text{C}$ for the solutions of $\text{AlCl}_3/\text{RR}'\text{SO}_2 = 1/4$ (mol) are shown in the Fig. 4a, 4b, and 4c, respectively.

From Fig. 4a and 4b, we can infer the concentration of active Al complex Al_2Cl_7^- ($\delta = 92$ ppm) seems higher in EiPS and EsBS than the others. This is due to the different melting point (m.p.) of sulfones as shown in Table 1. In another word, we can say that at 80°C , sulfone with lower m.p. such as EiPS and EsBS, shifts the equilibrium of Eq. 1 to the right much more than that with higher m.p. does (EnPS and DnPS), which is similar to the influence of temperature.

On the other hand, in Fig. 4c, we can see that both EnPS and DnPS show higher coulombic efficiencies than those with the others (EiPS, EsBS), indicating that there's the other important

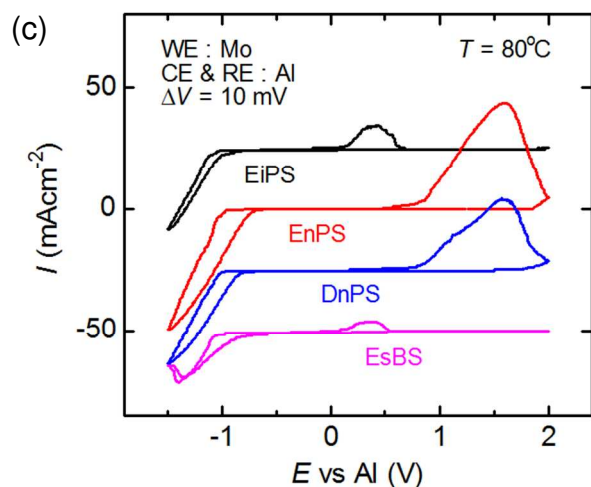
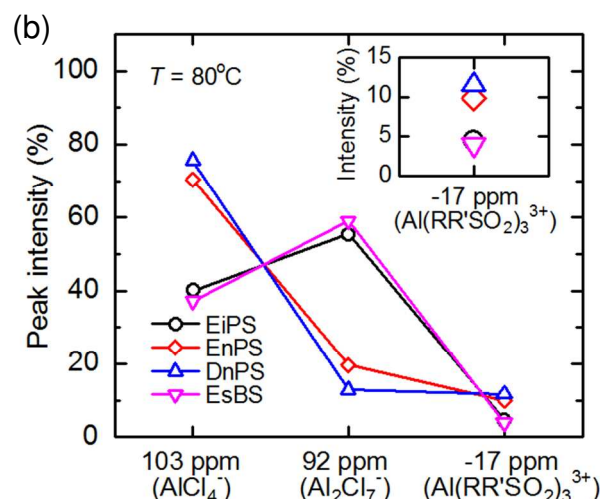
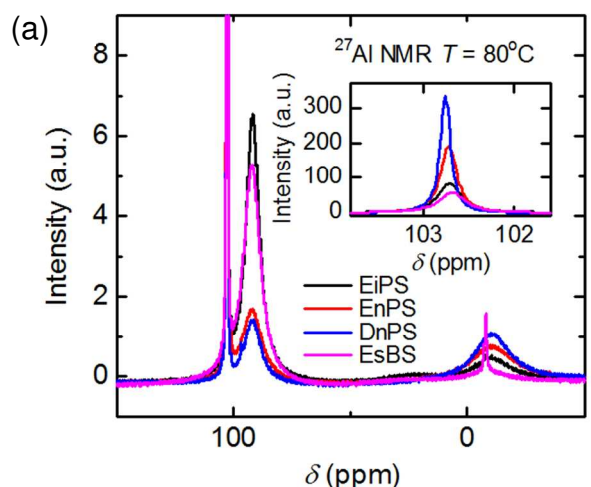


Fig.4 (a) ²⁷Al NMR spectra, (b) relative peak intensities, (c) and CV curves of $\text{AlCl}_3/\text{RR}'\text{SO}_2 = 1/4$ with various sulfones, EiPS (black), EnPS (red), DnPS (blue), and EsBS (pink). All measurements are performed at $T = 80^\circ\text{C}$. The inset in (a) shows an enlargement at $\delta = 103$ ppm, while that in (b) shows an enlargement for $\delta = -17$ ppm.

factor affecting the electrochemical activity than the concentration of Al_2Cl_7^- .

Here it should be noted that peak intensities at $\delta = -17$ ppm are

obviously larger in the electrolytes with both EnPS and DnPS than the others (Fig. 4b), which is not the effect of different m.p., but that of sulfones, as these peak intensities are not affected by temperature (Fig. 1c).

5 We think that the peak intensity at $\delta = -17$ ppm, or the stability of $\text{Al}(\text{RR}'\text{SO}_2)_3^{3+}$ is the essential factor for the electrochemical activities of the electrolyte. Formation of $\text{Al}(\text{RR}'\text{SO}_2)_3^{3+}$ provide excess Cl^- into the solution, allowing the equilibrium (1) that can proceed the reversible Al deposition and dissolution.^{6,13}

10

Aluminium chloride concentrations

It has been reported that there is a fast reaction following an equation



15 which allows us to expect higher Al_2Cl_7^- proportion by increasing AlCl_3 concentrations.^{4,13,15} Based on this concept, in order to realize the electrochemical activities at room temperature, we tried to increase the AlCl_3 concentrations in the solution. There was an interesting sulfone-dependence in the electrolyte 20 preparations; using EnPS or DnPS, we can get the solution with the composition up to $\text{AlCl}_3/\text{RR}'\text{SO}_2 = 3/2$ (mol), while $\text{AlCl}_3/\text{RR}'\text{SO}_2 = 1/1$ (mol) was the highest when we use EiPS as solvent. So we used EnPS as one of the best sulfones instead of EiPS to improve the electrochemical activity.

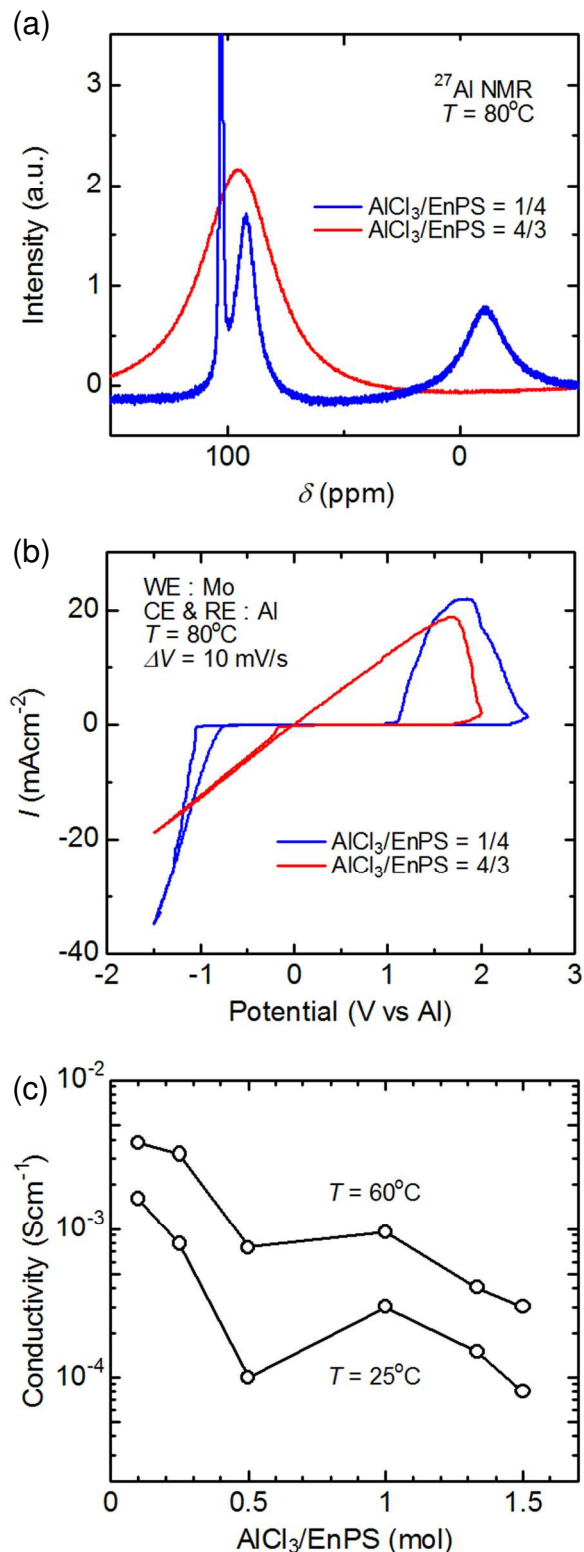
25 Figure 5a shows the ^{27}Al -NMR spectra taken at 80°C for a couple of Al electrolytes with different AlCl_3 concentrations, $\text{AlCl}_3/\text{EnPS} = 1/4$, and $4/3$. It is clearly found that, by increasing AlCl_3 concentration the major Al species has been changed from AlCl_4^- to Al_2Cl_7^- , which was accompanied by a drastic 30 improvement of electrochemical activities presented in Fig. 5b, where we can see reversible Al deposition and dissolution without over potentials for $\text{AlCl}_3/\text{EnPS} = 4/3$. Here it has been found that observed over potential is due to the low concentration of AlCl_3 , or the lack of electrochemically active Al complex 35 species.

Ionic conductivities of these Al electrolytes are plotted in Fig. 5c as a function of molar ratio $\text{AlCl}_3/\text{EnPS}$ that corresponds to AlCl_3 concentrations. Basically, conductivity decreases with increasing AlCl_3 concentration as the viscosity of solutions 40 increases. It should be noted that there are dips in the slopes around $\text{AlCl}_3/\text{EnPS} = 1/2$, or in another word, the abnormal increases of conductivities are observed between $\text{AlCl}_3/\text{EnPS} = 1/2$ and $1/1$. This is due to an unusual decrease of viscosity with increasing AlCl_3 concentration, which is so-called ionic liquid 45 behavior. Since major Al anions crossover from monomer (AlCl_4^-) to dimer (Al_2Cl_7^-) around $\text{AlCl}_3/\text{EnPS} = 1/2$, coulombic interaction between anions and cations ($\text{Al}(\text{EnPS})_3^{3+}$) get weakened resulting in a lower viscosity of the solutions. As far as we know, this is the first observation of bipolar-type ionic liquid 50 composed of Al anions and Al cations.

Dilutions

Despite the improvement of electrochemical activity presented in Fig. 5b, the operating temperature was still 80°C . In order to 55 make it active at 25°C , we tried to reduce the viscosity by

dilution.



60

Fig.5 AlCl_3 -concentration dependence of NMR spectra and electrochemical properties of sulfone-based Al electrolytes. (a) ^{27}Al NMR spectra and (b) CV curves of $\text{AlCl}_3/\text{EnPS} = 1/4$ (blue) and $4/3$ (red) observed at $T = 80^\circ\text{C}$. (c) Conductivities as a function of molar ratio of 65 $\text{AlCl}_3/\text{EnPS}$ observed at $T = 25^\circ\text{C}$ and 60°C . Dips at $\text{AlCl}_3/\text{EnPS} = 0.5$ represent the crossover point of major anions between AlCl_4^- ($\text{AlCl}_3/\text{EnPS} < 0.5$) and Al_2Cl_7^- (> 0.5).

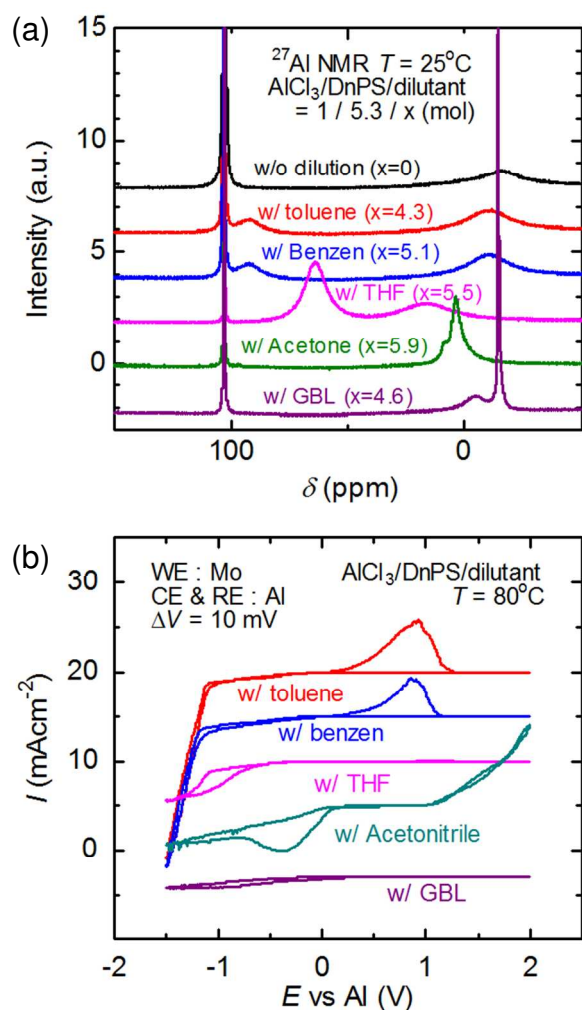


Fig.6 (a) ^{27}Al NMR spectra observed at $T = 25^\circ\text{C}$ for Al electrolytes $\text{AlCl}_3/\text{DnPS}/\text{dilutants} = 1/5.3/x$ (molar ratio) with various organic solvents as dilutants; toluene, benzene, THF, Acetone and GBL. (b) CV curves for each Al electrolytes observed at $T = 80^\circ\text{C}$.

Then, we measured ^{27}Al -NMR spectra after putting various organic solvents into the Al electrolytes of $\text{AlCl}_3/\text{DnPS}$ to find the materials that can be used as dilutants.

Figure 6a shows ^{27}Al -NMR spectra observed at $T = 25^\circ\text{C}$ for sulfone-based Al electrolytes diluted by various organic solvents as $\text{AlCl}_3/\text{DnPS}/\text{dilutants} = 1/5.3/x$ (mol), where x corresponds the molar ratio for each solvents as described in the figure. It has been found that dilutions by non-polar organic solvents having small dielectric constant (ϵ_r), such as benzene ($\epsilon_r = 2.27$) and toluene (2.38), can keep the spectra or Al ionic species stable, while polar solvents with large ϵ_r , such as tetrahydrofuran (THF, $\epsilon_r = 7.58$), acetone (20.6), and gamma-butyrolactone (GBL, 39.1), interact with the Al complexes, changing the NMR spectra drastically. It should be noted that introduction of non-polar organic solvents brings about small peaks at $\delta = 92$ ppm (corresponding to Al_2Cl_7^-), which means decent dilution has the same effect of raising temperature as shown in Fig. 1b, that is shifting the equilibrium (1) to the right. Here we should mention that there's no serious interaction between decent dilutants and

active Al complexes as the chemical shift of their Al-NMR peaks do not change with the dilution. (see Fig. S2 in supporting information)

CV curves for $\text{AlCl}_3/\text{DnPS}/\text{dilutants} = 1/5.3/x$ (mol) observed at $T = 80^\circ\text{C}$ are described in Fig. 6b, where we can see the Al deposition and dissolution only when the electrolyte was diluted by non-polar solvents. From these results, we have chosen toluene as an appropriate dilutant for the sulfone-based Al electrolytes.

Optimizations

Using toluene as a dilutant, we have successfully reduced the viscosities and expanded the stable compositions of the electrolytes. Prepared solutions are plotted on a ternary phase diagram together with their information of electrochemical activities at $T = 25^\circ\text{C}$ in Fig. 7a. Al electrolytes whose compositions are plotted in yellow region showed reversible Al deposition and dissolution at room temperature, and those within the blue region are preferable as their over potentials are small.

Three Al electrolytes are selected for examples, whose compositions are marked by filled circles in Fig. 7a that are $\text{AlCl}_3/\text{EnPS}/\text{Toluene} = 1/1.2/2.9$, $1/1/2.9$, and $1/0.6/2.9$ (mol). Their ^{27}Al -NMR spectra observed at 25°C are shown in Fig. 7b. From this figure, it is easily found that Al_2Cl_7^- exists in all electrolytes at 25°C , which allows us to expect the reversible Al deposition and dissolution at room temperature. In addition, we can see that the proportion of Al_2Cl_7^- to AlCl_4^- is increased successively with increasing AlCl_3 concentration. Although the peaks of $\text{Al}(\text{EnPS})_3^{3+}$ are too small to see in this figure at $\delta = -17$ ppm, their existence was confirmed by the Fourier transform infrared (FT-IR) measurements, whose spectra were presented in Fig. 7c. Al electrolytes of $\text{AlCl}_3/\text{EMICl} = 1/1$, and $2/1$ (mol), as well as $\text{Al}(\text{BF}_4)_3/\text{EnPS} = 1/8$ (mol) were also measured as references to identify the Al ionic species AlCl_4^- , Al_2Cl_7^- , and $\text{Al}(\text{EnPS})_3^{3+}$, respectively.

Specific vibrations were observed at 490 cm^{-1} for $\nu_{\text{Al-Cl}}$ of AlCl_4^- , 550 cm^{-1} for $\nu_{\text{Al-Cl}}$ of Al_2Cl_7^- ,¹⁶ and 620 cm^{-1} for $\nu_{\text{Al-O}}$ of $\text{Al}(\text{EnPS})_3^{3+}$.¹⁷ It is clear that, with increasing AlCl_3 concentration, AlCl_4^- decreases while Al_2Cl_7^- increases, which is consistent with the results of ^{27}Al -NMR measurements (Fig. 7b). And in addition, it is noteworthy that peaks corresponding to $\nu_{\text{Al-O}}$ of $\text{Al}(\text{EnPS})_3^{3+}$ were observed in all electrolytes. This is an evidence that Al cations $\text{Al}(\text{RR}'\text{SO}_2)_3^{3+}$ always exist in the sulfone-based Al electrolytes irrespective of AlCl_3 concentrations.

And as expected, Figure 7d represents the reversible Al deposition and dissolution observed at 25°C . Here we can identify the active Al species of each specific reaction having different over potentials by comparing CV curves with NMR spectra between Figs. 7b and 7d. It has been demonstrated that Al deposition is ruled by Al_2Cl_7^- , while Al dissolution is subject to AlCl_4^- , both of which are maintained by the equilibrium of the Equation (1).

Cite this: DOI: 10.1039/c0xx00000x

www.rsc.org/xxxxxx

FULL PAPER

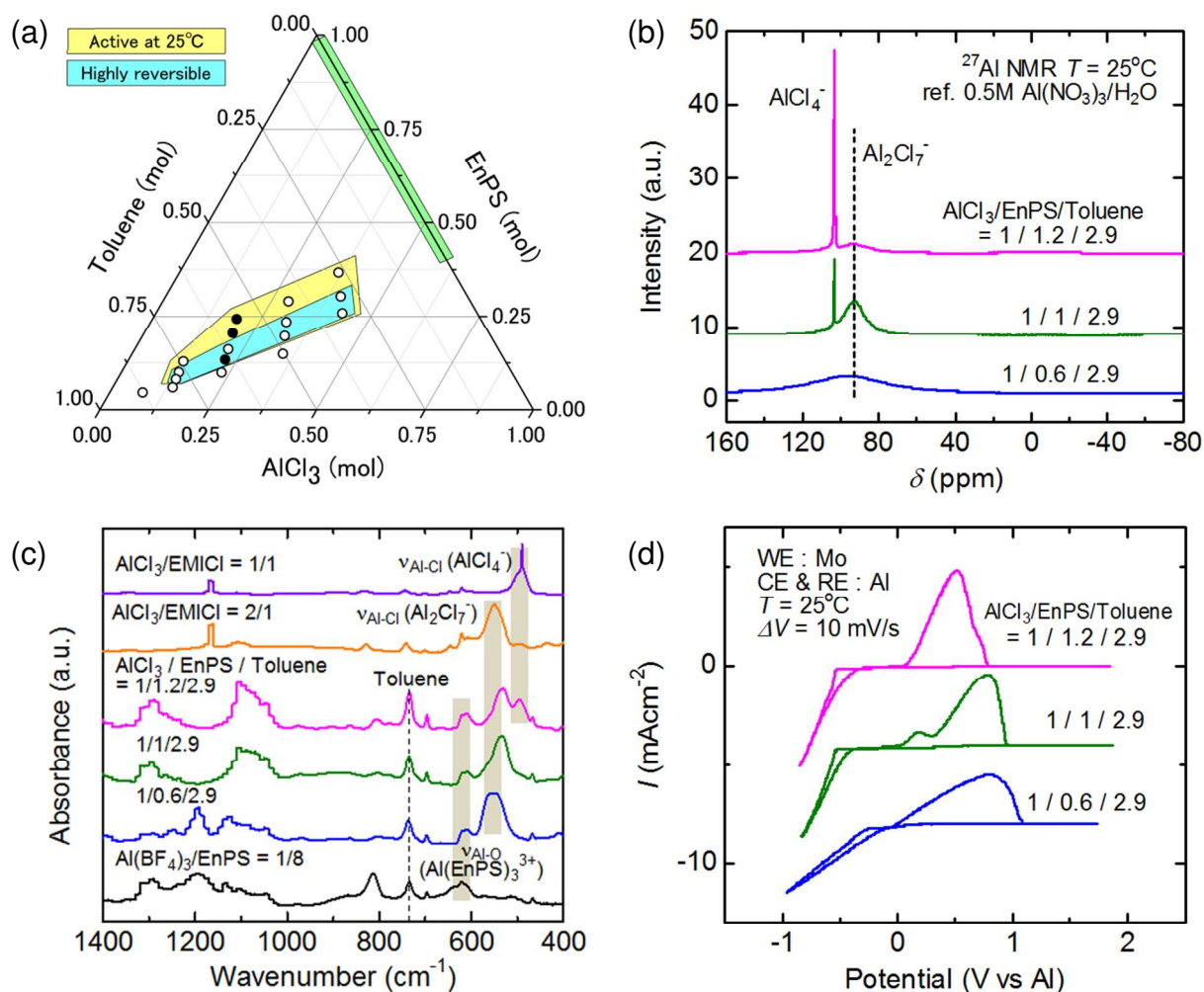


Fig.7 Improvements of sulfone-based Al electrolytes observed at $T = 25^\circ\text{C}$. (a) Ternary phase diagram for Al electrolytes of $\text{AlCl}_3/\text{EnPS}/\text{Toluene}$ (molar ratio). A green line shows the available compositions without toluene, representing the validity of dilutions. Regarding the solutions with the compositions plotted in a yellow region, reversible Al depositions and dissolutions were observed, while those in a blue region are preferred as the over potentials are small. (b) ^{27}Al NMR spectra, (c) FT-IR spectra and (d) CV curves of sulfone-based Al electrolytes $\text{AlCl}_3/\text{EnPS}/\text{Toluene} = 1/1.2/2.9$, $1/1/2.9$, and $1/0.6/2.9$, whose compositions are plotted as filled circles in Fig.7a. Reference electrolytes are also presented in Fig.7c, where vibrations characteristic for three Al ionic species are observed at 490 cm^{-1} ($\nu_{\text{Al-Cl}}$ of AlCl_4^-), 550 cm^{-1} ($\nu_{\text{Al-Cl}}$ of Al_2Cl_7^-), and 620 cm^{-1} ($\nu_{\text{Al-O}}$ of $\text{Al}(\text{EnPS})_3^{3+}$). Dashed line represents a specific vibration for toluene.

10

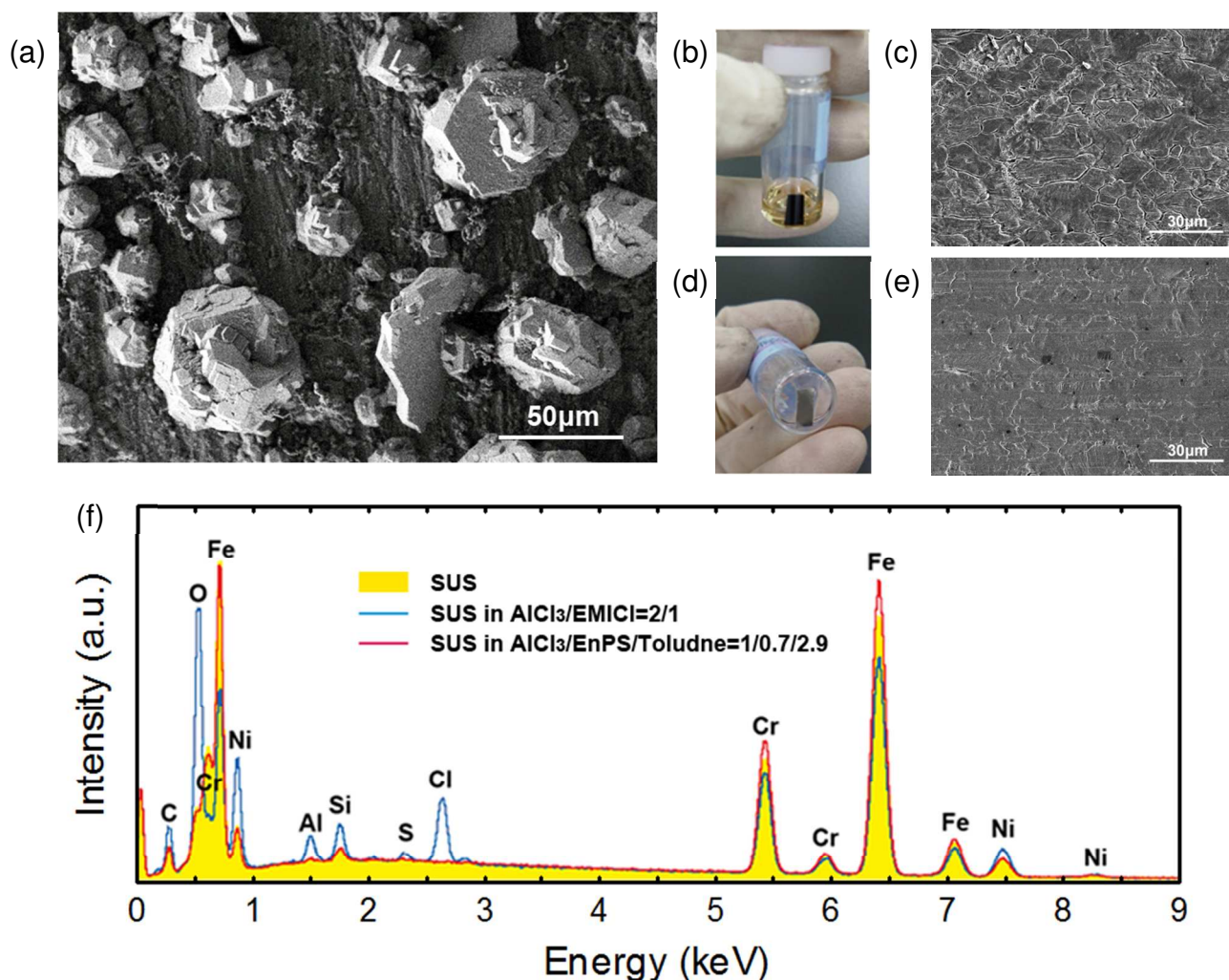


Fig.8 (a) SEM image of Al metals deposited on Al counter electrode from AlCl₃/EnPS/Toluene = 1/0.7/2.9 (mol). (b-f) Comparison of stainless steel strips soaked in Al electrolytes by photographs (b,d), SEM images (c,e), and EDX spectra (f), where yellow spectrum represents the original stainless steel (SUS). (b,c,f) In the case of AlCl₃/EMICl = 2/1 (mol), the stainless steel get colored and roughness increases involving Cl and O on the surface. (d,e,f) On the other hand, regarding AlCl₃/EnPS/Toluene = 1/0.7/2.9, the stainless steel does not show any drastic change of the surfaces after soaking in the electrolyte.

Morphologies of deposited aluminium and electrolyte corrosions

Morphology of electrodeposited Al is an important issue for the development of Al metal anodes. As far as we use the sulfone-based Al electrolytes, deposited Al always shows bulk rock-like morphology and dendrite formation has never been observed irrespective of the compositions or the current densities. Figure 8a shows the typical scanning electron microscope (SEM) image of Al metal deposited on the Al electrode from the sulfone-based Al electrolytes AlCl₃/EnPS/Toluene = 1/0.7/2.9 (mol) at $T = 25^{\circ}\text{C}$. Thanks to this morphology, we can expect the relevant cyclic efficiency as well as the safety without dendrite formation.

Another important issue for the development of Al electrolytes is their corrosion properties. The simple way to check the corrosion is just to soak the stainless steel strips in Al electrolytes, whose results are presented in Figs. 8b-f. In the case of ionic liquid AlCl₃/EMICl = 2/1, the strip got colored after 24h steep with increasing surface roughness. It should be noted that in the spectra of energy dispersive X-ray spectroscopy (EDX) in Fig.

8f, the peak intensities of oxygen (O) and chloride (Cl) increased while those of iron (Fe) and chromium (Cr) decreased after soaking. On the other hand, regarding the sulfone-based Al electrolyte AlCl₃/EnPS/Toluene = 1/0.7/2.9, the strip keeps shining without roughness increase nor the compositional change at the surface. This feature allows us to use the electrolytes in general coin cells as well as in pouch cells, since they are not corrosive.

This corrosion-free property of the sulfone-based Al electrolyte is due to the relatively low concentration of AlCl₃ involved in the solution. Actually, reversible Al deposition and dissolution is realized at 25°C using AlCl₃/EnPS/Toluene = 1/0.6/5.8 (mol), where AlCl₃ concentration is smaller than 1.5 mol/L, which is less than 1/4 of conventional ionic liquids like AlCl₃/EMICl = 2/1 whose AlCl₃ concentration is larger than 6 mol/L.^{13,18} We think that the origin of these characteristics is the stability of solvated Al cation Al(EnPS)₃³⁺ that does not work in itself, but keeps the above equilibrium (1) by releasing 3 Cl⁻ in the solutions, which is essential for the electrochemical activity of sulfone-based Al electrolyte.

Conclusions

Non-corrosive Al electrolytes working at room temperature have been successfully developed using AlCl_3 , dialkylsulfone, and dilutants. We have observed Al complex species in the electrolytes, and revealed that Al deposition is ruled by Al_2Cl_7^- , and Al dissolution is subject to AlCl_4^- , while $\text{Al}(\text{RR}'\text{SO}_2)_3^{3+}$ is inactive. Dialkylsulfones not only play as solvents but also decide the stability of Al complexes $\text{Al}(\text{RR}'\text{SO}_2)_3^{3+}$ that rule the essential equilibrium inside the solutions. We can control the electrochemical activities by managing AlCl_3 concentrations together with the non-polar organic solvents as dilutants. Al dendrites have never been observed in the Al deposition as far as the electrolytes are used. Consequently, we can make use of Al metal anodes at ambient conditions using sulfone-based Al electrolytes, by which the doors are opened for the development of Al rechargeable batteries.

Supporting information

Supporting Information is available online from the RSC or from the authors.

Acknowledgements

The authors wish to thank Dr. Kazuhiro Noda and Yoshio Nishi for their fruitful supports, and Dr. Toshimi Fukui for valuable discussions. We are also grateful to Dr. Yoshinori Kitajima for his kind cooperation on XAFS experiments.

Notes and references

^a Advance Materials Laboratories, Sony Corporation, Atsugi Tec. 4-14-1 Asahi-cho, Atsugi-shi, Kanagawa, 243-0014, Japan. Fax: +81 50 3809 1406; Tel: +81 50 3141 1792; E-mail: yuri.nakayama@jp.sony.com

^b Energy Materials Research Laboratory, KRI, Inc., Kyoto Research Park, 134, Chudoji Minami-machi, Shimogyo-ku, Kyoto 600-8813, Japan

- 1 M. Armand, J. M. Tarascon, *Nature* **2008**, 451, 652.
- 2 P. Yang, J. M. Tarascon, *Nat. Mater.* **2012**, 11, 560.
- 3 Q. Li, N. J. Bjerrum, *J. Power Sources* **2002**, 110, 1.
- 4 J. S. Wilkes, J. A. Levisky, R. A. Wilson, C. L. Hussey, *Inorg. Chem.* **1982**, 21, 1263; J. J. Auburn, Y. L. Barberio, *J. Electrochem. Soc.* **1985**, 132, 598; Y. Zhao, T. J. VanderNoot, *Electrochim. Acta* **1997**, 42, 3; T. Jiang, M. J. Chollier Brym, G. Dube, A. Lasia, G. M. Brisard, *Surf. Coat. Tech.* **2006**, 201, 1.
- 5 N. Koura, H. Ejiri, K. Takeishi, *J. Electrochem. Soc.* **1993**, 140, 602; N. Jayaprakash, S. K. Das, L. A. Archer, *Chem. Comm.* **2011**, 47, 12610; J. V. Rani, V. Kanakaiyah, T. Dadmal, M. S. Rao, S. Bhavanarushi, *J. Electrochem. Soc.* **2013**, 160, A1781; W. Wang, B. Jiang, W. Xiong, H. Sun, Z. Lin, L. Hu, J. Tu, J. Hou, H. Zhu, S. Jiao, *Sci. Reports* **2013**, 3, 3383.
- 6 C. -H. Tseng, J. -K. Chang, J. -R. Chen, W. T. Tsai, M. -J. Deng, I. -W. Sun, *Electrochem. Comm.*, **2010**, 12, 1091.
- 7 L. D. Reed, E. Menke, *J. Electrochem. Soc.* **2013**, 160, A915.
- 8 L. Legrand, A. Tranchant, R. Messina, *Electrochim. Acta* **1994**, 39, 1427; L. Legrand, A. Tranchant, R. Messina, *J. Electrochem. Soc.* **1994**, 141, 378; L. Legrand, M. Heintz, A. Tranchant, R. Messina, *Electrochim. Acta* **1995**, 40, 1711; L. Legrand, A. Tranchant, R. Messina, *Electrochim. Acta* **1996**, 41, 2715; L. Legrand, A. Tranchant, R. Messina, F. Romain, A. Lautie, *Inorg. Chem.* **1996**, 35, 1310; L. Legrand, A. Chausse, R. Messina, *Electrochim. Acta* **2001**, 46, 2407.
- 9 T. Jiang, M. J. Chollier Brym, G. Dube, A. Lasia, G. M. Brisard, *Surf. Coat. Tech.* **2007**, 201, 6309.

- 10 Y. Kitajima, Y. Yonamoto, K. Amemiya, H. Tsukabayashi, T. Ohta, K. Ito, *J. Elec. Spec. Rel. Phen.*, **1999**, 101-103, 927.
- 11 Y. Nakayama, Y. Kudo, H. Oki, K. Yamamoto, Y. Kitajima, K. Noda, *J. Electrochem. Soc.*, **2008**, 155, A754.
- 12 J. S. Wilkes, J. S. Frye, G. F. Reynolds, *Inorg. Chem.* **1983**, 22, 3870.
- 13 S. Schaltin, M. Ganapathi, K. Binnemans, J. Fransaera, *J. Electrochem. Soc.* **2011**, 158, D634.
- 14 K. Xu, C. A. Angell, *J. Electrochem. Soc.* **2002**, 149, A920.
- 15 N. Koura, M. Murase, *Light Metals* **1989**, 39, 333.
- 16 R. J. Gale, R. A. Osteryoung, *Inorg. Chem.*, **1980**, 19, 2240.
- 17 L. Andrews, T. R. Burkholder, J. T. Yustein, *J. Phys. Chem.* **1992**, 96, 10182.
- 18 Z. J. Karpinski, R. A. Osteryoung, *Inorg. Chem.* **1985**, 24, 2259.